4.1.2.2 Solar activity cycle

Sami Solanki, Natalie Krivova

4.1.2.2.1 The sunspot cycle

Cyclicity in the number of sunspots on the solar disc with a period of roughly 10 years was discovered by Heinrich Schwabe after 17 years of observations [44Sch, c]. To explore this further, Rudolf Wolf initiated in 1848 systematic daily observations of sunspots, collected available data back to 1700 and introduced a quantitative measure of sunspot activity. The Relative (also called Zurich, International or Wolf) Sunspot Number is defined as

$$R_{\mathrm{Z}} = k(10g + s), \tag{1}$$

where g is the number of sunspot groups, s is the total number of individual spots and k is a factor that depends on the observer. Each daily sunspot number is computed as a weighted average of a number of individual measurements. Only monthly averaged data are available for the period 1749-1817, and only yearly averages prior to 1749.

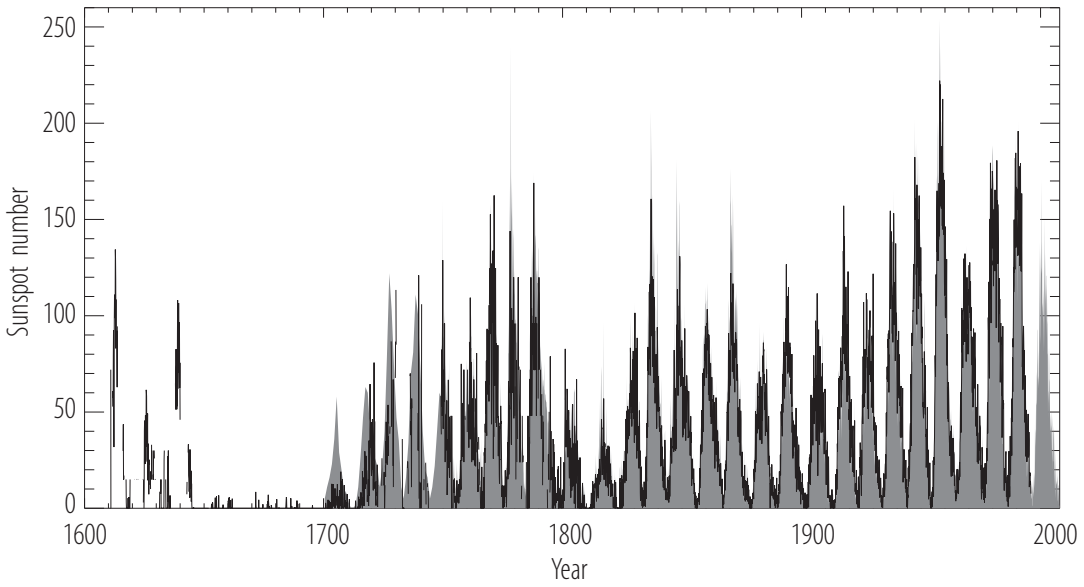

Fig. 1. Monthly averaged Group (black solid line) and Zurich (grey shaded area) sunspot numbers. Only yearly values of the Zurich number are available in the period 1700-1749.

Hoyt & Schatten [98Hoy] introduced the Group Sunspot Number (GSN, R_{G}) as a less seeing-dependent and noisy alternative to the Wolf Sunspot Number. Wolf's sunspot number is affected by the size limit of the detected sunspots. The better the seeing conditions, the larger the obtained value. The GSN uses only the number of sunspot groups observed, rather than groups and individual sunspots:

$$R_{\mathrm{G}} = \frac{12.08}{N} \sum k_i' G_i, \tag{2}$$

where G_i is the number of sunspot groups recorded by the i-th observer, k_i' is the i-th observer's correction factor, N is the number of observers used to form the daily value, and 12.08 is a

normalisation factor chosen to make the mean R_G identical with the mean R_Z for the period 1874 to 1976. The GSN record of daily measurements goes back to 1610 and additionally supplies data for more than 45 000 individual days prior to 1874 not included in the R_Z set. Monthly values of R_Z (yearly in the period between 1700 and 1749) and R_G are shown in Fig. 1. The data are available from the National Geophysical Data Center (NGDC) [08Nat].

The length and the strength of the sunspot cycle vary with time (Fig. 1 and Table 1). The length of the cycle changes in the range between approximately 9 and 14 years [99Fli]. Weaker cycles tend to be somewhat longer although more clearly the cycles preceding weak cycles tend to be longer [94Hat, 02Hat, 03Sol]. Waldmeier [35Wal] also found that the length of the ascending phase of a cycle ('rise time') is anti-corellated with the maximum sunspot number of that cycle (Waldmeier's law). However, whereas the correlation is quite pronounced (correlation coefficient, r_c, is about -0.7) for the Wolf's number, it is relatively weak ($r_c \approx -0.3$) for the GSN [02Hat] and is absent for the sunspot area [08Dik].

Sunspots typically appear as pairs (or small groups), with the leading spot(s) showing opposite magnetic polarity to the following one(s). The polarities of preceding or following spots are the same in a given hemisphere. They are opposite to each other in the northern relative to the southern hemisphere, and they reverse from one cycle to another [19Hal] (Hale's polarity law), so that the full magnetic activity cycle has a period of about 22 years (Hale cycle; [c]). A tendency has been observed for odd cycles (in the traditional numbering, see Table 1) to be stronger than the preceding even cycles (Gnevyshev-Ohl rule; [48Gne]), although occasionaly this rule breaks down, e.g. in cycle pairs 4/5, 8/9 or 22/23 (see Table 1 and [07Cha]).

The axes joining the leading and following parts of active regions are tilted on average such that the leading spots lie slightly equatorward of the following spots. The average tilt angle is about 4-5° but it increases from 0° near the equator to about 12° at 30° latitude (Joy's law; [19Hal, 91How]).

Not only the total number of spots vary over the cycle but also other parameters [f, a]. In 1874 the Royal Greenwich Observatory in the UK started routine monitoring of sunspot regions moving across the solar disc. A number of parameters were recorded daily, such as the number of spots and their groups, positions, total area of umbrae, penumbrae and faculae. Observed (projected onto the disc) areas measured in millionths of the solar disc are corrected for the foreshortening effect using measured positions of spots, in order to calculate sunspot areas in millionths of the solar hemisphere (corrected areas). The Greenwich Observatory programme ceased in 1976. During different periods of time, similar programmes were carried out by the US Air Force (USAF), Russian and Debrecen (Hungary) networks, and a number of individual observatories, including Mt. Wilson (USA, later part of the USAF network), Rome (Italy), Taipei (Taiwan), Catania (Italy), Yunnan (China) etc. (see [08Nat] for data). Sunspot areas measured at different stations show systematic differences and have to be cross-calibrated when compiling a complete time series [05Bal].

Total area covered by sunspots as well as the latitudes at which they emerge vary systematically over the solar cycle. Sunspots are typically seen within an equatorial belt ('activity belt') between $-35°$ south and $+35°$ north latitude. At the beginning of a new solar cycle, sunspots appear first at higher latitudes (above $\approx |25|°$), but as the cycle progresses the spots migrate towards lower latitudes resulting in a 'butterfly' pattern of the latitudes vs. time (butterfly or Maunder's [58Car, 04Mau] diagram, also Spoerer's law; Fig. 2). The latitudinal drift is about 2-4° per year at the beginning of the cycle, when the average spot latitudes are $\gtrsim |15|$, slowing down to about 1° at lower latitudes. At a latitude of about 8°, the equatorward drift stops [03Hat]. Cycles with larger drift velocities at cycle maximum ($\gtrsim 2$ deg/a) tend to be shorter ($\lesssim 10.5$ a) and stronger [03Hat].

The mean latitude, $\langle l \rangle$ at which sunspots are located during a given cycle was 14.95 ± 1.34 for cycles 12-22, and it varied by a factor of about 1.5 from one cycle to another [08Sol]. Stronger cycles have sunspots on average at higher latitudes and distributed over a wider range of latitudes [08Sol]. As $\langle l \rangle$ shifts poleward by 5°, the width of the latitude distribution increases by 2°.

Table 1. Epochs of sunspot maxima and minima, cycle length and the largest smoothed monthly mean sunspot number. Dates of cycle minima and maxima are based on averages of the corresponding time extremes reached in the monthly mean sunspot number, in the smoothed monthly mean sunspot number, and in the monthly mean number of spot groups alone. Two more measures are used to determine times of sunspot minima: the number of spotless days and the frequency of occurrence of 'old' and 'new' cycle spot groups [08Nat]. The smoothed monthly mean sunspot number is defined as the arithmetic average of two sequential 12-month running means of monthly mean numbers. Earlier, significantly less reliable data are marked by asterisks. The value of the cycle length for cycle 23 is a preliminary rough estimate.

Cycle number	Min. epoch	Max. epoch	Cycle length [a]	Max. SN	Cycle number	Min. epoch	Max. epoch	Cycle length [a]	Max. SN
–	1610.8*	1615.5*	8.2*		6	1810.6	1816.4	12.7	48.7
–	1619.0*	1626.0*	15.0*		7	1823.3	1829.9	10.6	71.7
–	1634.0*	1639.5*	11.0*		8	1833.9	1837.2	9.6	146.9
–	1645.0*	1649.0*	10.0*		9	1843.5	1848.1	12.5	131.6
–	1655.0*	1660.0*	11.0*		10	1856.0	1860.1	11.2	97.9
–	1666.0*	1675.0*	13.5*		11	1867.2	1870.6	11.7	140.5
–	1679.5*	1685.0*	10.0*		12	1878.9	1883.9	10.7	74.6
–	1689.5*	1693.0*	8.5*		13	1889.6	1894.1	12.1	87.9
–	1698.0*	1705.5*	14.0*		14	1901.7	1907.0	11.9	64.2
–	1712.0*	1718.2*	11.5*		15	1913.6	1917.6	10.0	105.4
–	1723.5*	1727.5*	10.5*		16	1923.6	1928.4	10.2	78.1
–	1734.0*	1738.7*	11.0*		17	1933.8	1937.4	10.4	119.2
–	1745.0*	1750.3	10.2	92.6	18	1944.2	1947.5	10.1	151.8
1	1755.2	1761.5	11.3	86.5	19	1954.3	1957.9	10.6	201.3
2	1766.5	1769.7	9.0	115.8	20	1964.9	1968.9	11.6	110.6
3	1775.5	1778.4	9.2	158.5	21	1976.5	1979.9	10.3	164.5
4	1784.7	1788.1	13.6	141.2	22	1986.8	1989.6	9.7	158.5
5	1798.3	1805.2	12.3	49.2	23	1996.4	2000.3	(∼12.3)	120.8

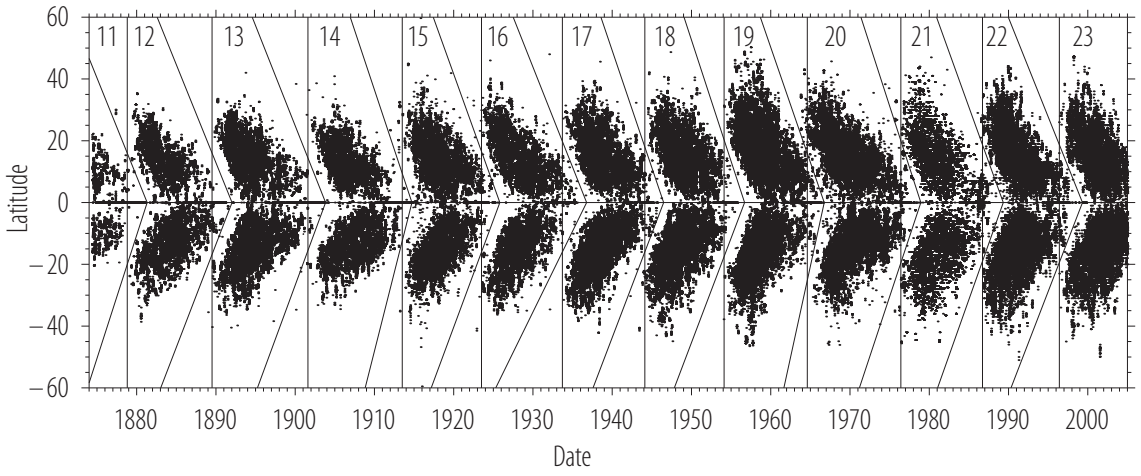

Fig. 2. Butterfly diagram [08Sol]. The vertical dashed lines mark the official minima of the sunspot cycle (Table 1), the inclined solid lines are estimates of the boundaries between individual cycles by [08Sol]. Cycle numbers are given at the top of each cycle.

4.1.2.2.2 The magnetic cycle

Regular measurements of the solar global photospheric magnetic field commenced in 1966, when daily synoptic full-disc magnetograms started being recorded at Mount Wilson [85How]. In the 1970s similar programmes were initiated at the National Solar Observatory on Kitt Peak [76Liv] and Wilcox Solar Observatory [77Sch]. The total (unsigned) photospheric flux for the period between 1974 and 2002 calculated by [02Arg] (NSO data were partly corrected by [06Wen]) from the magnetograms recorded at the three sites is shown in Fig. 3.

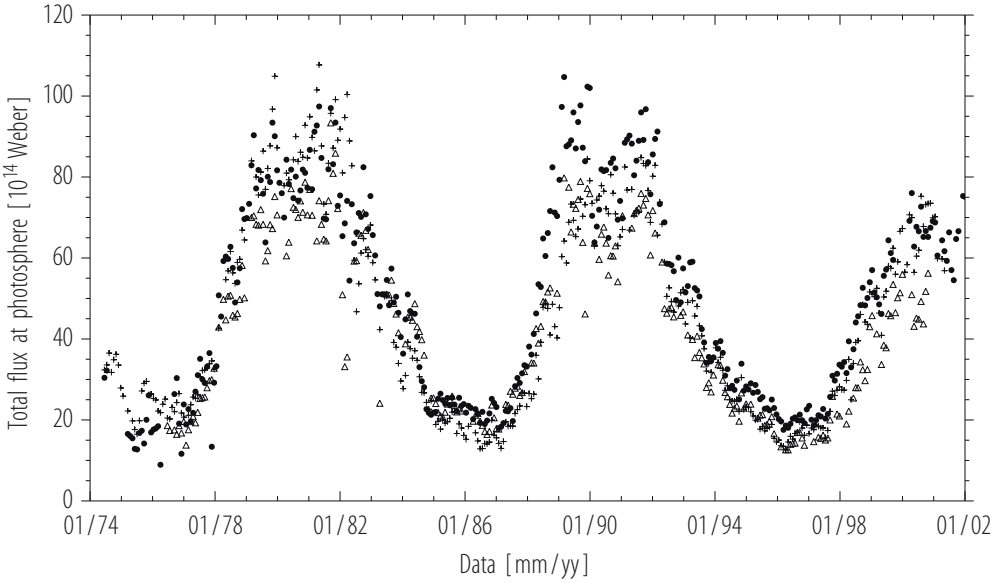

Fig. 3. Total (unsigned) photospheric flux for each Carrington rotation between 1974 and 2002 based on data from National (circles), Wilcox (plus signs) and Mount Wilson (triangles) Solar Observatories [02Arg, 06Wen].

The magnetic flux varies over the activity cycle and the maximum is reached about a year or two after the sunspot maximum. This variation mainly comes from the evolution of the active regions, whereas the total magnetic flux in the quiet Sun network varies from minimum to maximum by no more than a factor of 2 [b]. The total magnetic flux in the quiet Sun network exceeds that in active regions during activity minima [b] and is comparable to the active region flux at activity maxima [04Kri]. Since individual magnetic elements are small compared to the pixel sizes of magnetograms, at least half of the magnetic flux in the quiet Sun remains undetected due to the cancellation of the flux from opposite polarity elements present within the same pixel [04Kri]. Thus the actual total photospheric magnetic flux of the Sun is higher than Fig. 3 suggests.

The magnetic field emerges in the form of bipolar regions with total (unsigned) magnetic flux in the range about $5 \times 10^{20} - 5 \times 10^{22}$ Mx (active regions often harbouring sunspots and restricted to the active latitudes of 5-35° mainly) and $2 \times 10^{18} - 5 \times 10^{20}$ Mx (ephemeral active regions distributed up to latitudes of at least 60°) [b, 01Hag, 03Hag]. The distribution of the emergence latitudes gradually broadens with decreasing flux [b, 03Hag]. As in the case of sunspots, the leading and following polarities are the same in each hemisphere, opposite in the two hemispheres and reversed from one cycle to another (Hale's polarity law; see Fig. 4 and Sect. 4.1.2.2.1). In the course of the solar cycle, the emergence frequency of bipolar regions varies by a factor of 8 and 2 for larger (magnetic fluxes exceeding a few times 10^{20} Mx) and smaller (fluxes of a few times $10^{19} - 10^{20}$ Mx) regions, respectively [b, 03Hag]. For regions with fluxes below a few times

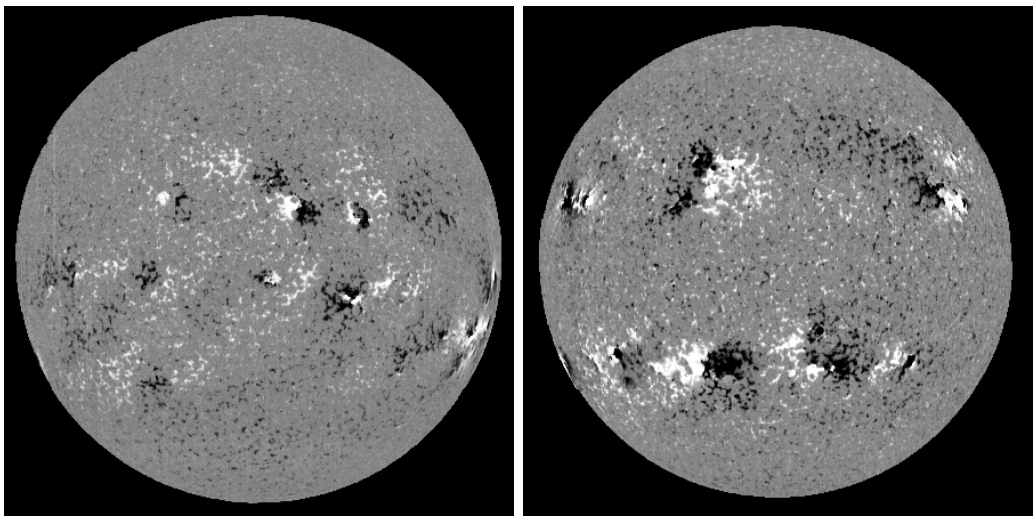

Fig. 4. KP NSO magnetograms (from http://synoptic.nso.edu/) taken on January 12, 1993 (cycle 22) and July 2, 1998 (cycle 23). White and black correspond to positive and negative magnetic polarities, respectively. Regions of strong magnetic fields are grouped in pairs of opposite polarities. The ordering of positive and negative regions is the same in a given hemisphere, opposite in the northern and southern hemispheres, and reverses from cycle 22 to 23.

10^{19} Mx, the emergence frequency is modulated even less, showing even a weak anticorrelation with the sunspot cycle [03Hag].

The latitude distribution of the photospheric magnetic field also displays the butterfly pattern ([b, 03Hat]; Fig. 5). Beside the equatorial drift of the active latitudes, also evident is a poleward meridional flow, leading to the polar field reversal from one cycle to another. The area covered by the polar fields and their total magnetic flux are maximal around cycle minimum. As the cycle progresses, meridional motions transport the following polarity magnetic elements seen on the poleward edges of the butterfly wings towards the poles with typical velocities of about 10 ms^{-1} [03Hat]. These large-scale unipolar fields, predominantly of opposite polarity to the polar fields, cancel with the magnetic fields in the polar regions. The polar fields shrink and then disappear for a few months to about a year before they reverse. The reversal is completed at different times in the northern and nouthern hemispheres. During the rest of the cycle, the polar fields build up reaching maximum flux by the next cycle minimum.

4.1.2.2.3 Irradiance and other parameters

Variations over the solar cycle in the area covered by sunspots, which appear dark on the solar surface (Sect. 4.1.2.3), and their bright counterparts, faculae and the network (Sect. 4.1.2.4), lead to variations in solar irradiance (Sect. 4.1.1.3.1). Sunspots on the visible hemisphere cause a darkening of the Sun by up to 0.2% on time scales of hours (for small very short-lived spots) to roughly a week (long-lived spots). The magnitude of the dip is approximately proportional to the projected area of the spot (see Sect. 4.1.2.3.2). Faculae and the network are responsible for the overall brightening by about 0.1% (for cycles 21-23) from activity minimum to maximum ([06Fro]; Fig. 6a).

Also the spectral distribution of the solar irradiance changes in the course of the activity cycle. The amplitude of the variation grows with decreasing wavelength (Table 2), reaching about 100% in the vicinity of the Ly-α emission line near 121.6 nm (see Fig. 6b; data from [00Woo]). About 60% of the total irradiance variations originate at wavelengths below 400 nm [06Kri]. Cyclic behaviour

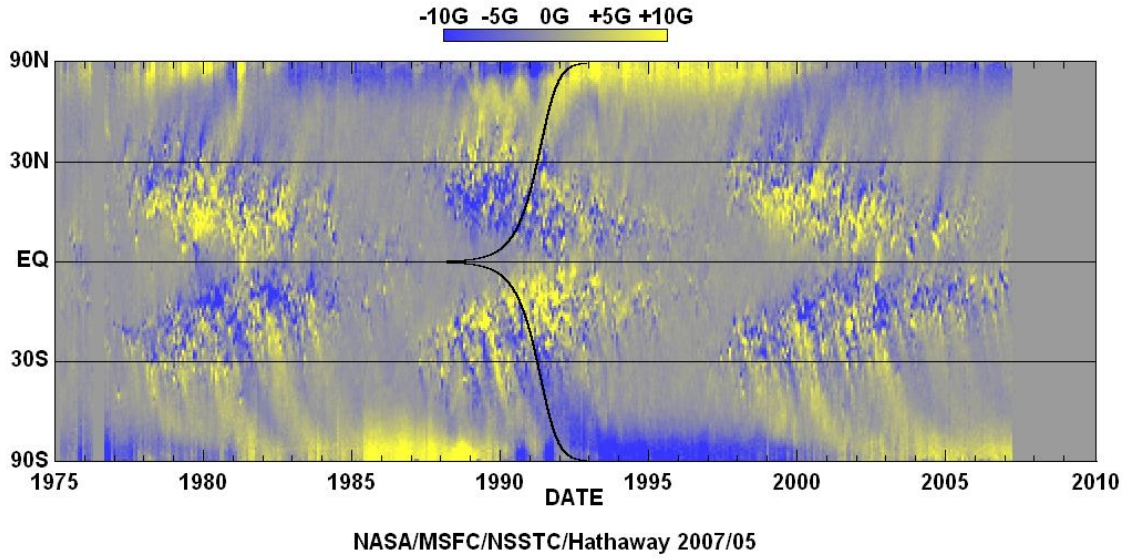

Fig. 5. (see color-picture part, page 615) Butterfly diagram of the radial component of the solar magnetic field [03Hat]. For each Carrington rotation, the magnetic flux is summed in longitude in each latitude bin.

Table 2. Amplitude of the solar cycle variation of solar spectral irradiance in the UV, visible and IR [00Unr, 03Flo, 06Kri].

Wavelength range [nm]	Variation, [%]
115-125	50-130
125-140	30-60
140-160	≈ 20
160-200	≈ 10
200-260	3-6
260-300	1-2
300-400	≈ 0.5
400-1000	≈ 0.01-0.1
1000-3000	negative
3000-10000	≈ 0.01-0.1
TSI	≈ 0.1

is also shown by many other proxies of solar activity including the Mg II core-to-wing ratio, solar radio flux at 10.7 cm, Ca K and He 1083 nm indices, among others.

The broad Mg II resonance lines in the solar spectrum (the h, 279.54 nm, and k, 280.23 nm, [e], emission doublet in the deepest parts of the 3 nm wide absorption feature formed by these lines) have been regularly monitored by a number of spaceborne instruments since 1978 [04Vie]. The brightness of the chromospheric emission cores changes significantly over the solar cycle, whereas the photospheric wings depend very weakly on solar activity. The Mg II index is thus defined as the ratio of the brightness in the emission core to that in the neighbouring continuum or wings. The ratio has the advantage that it is much less susceptible to instrumental trends than direct

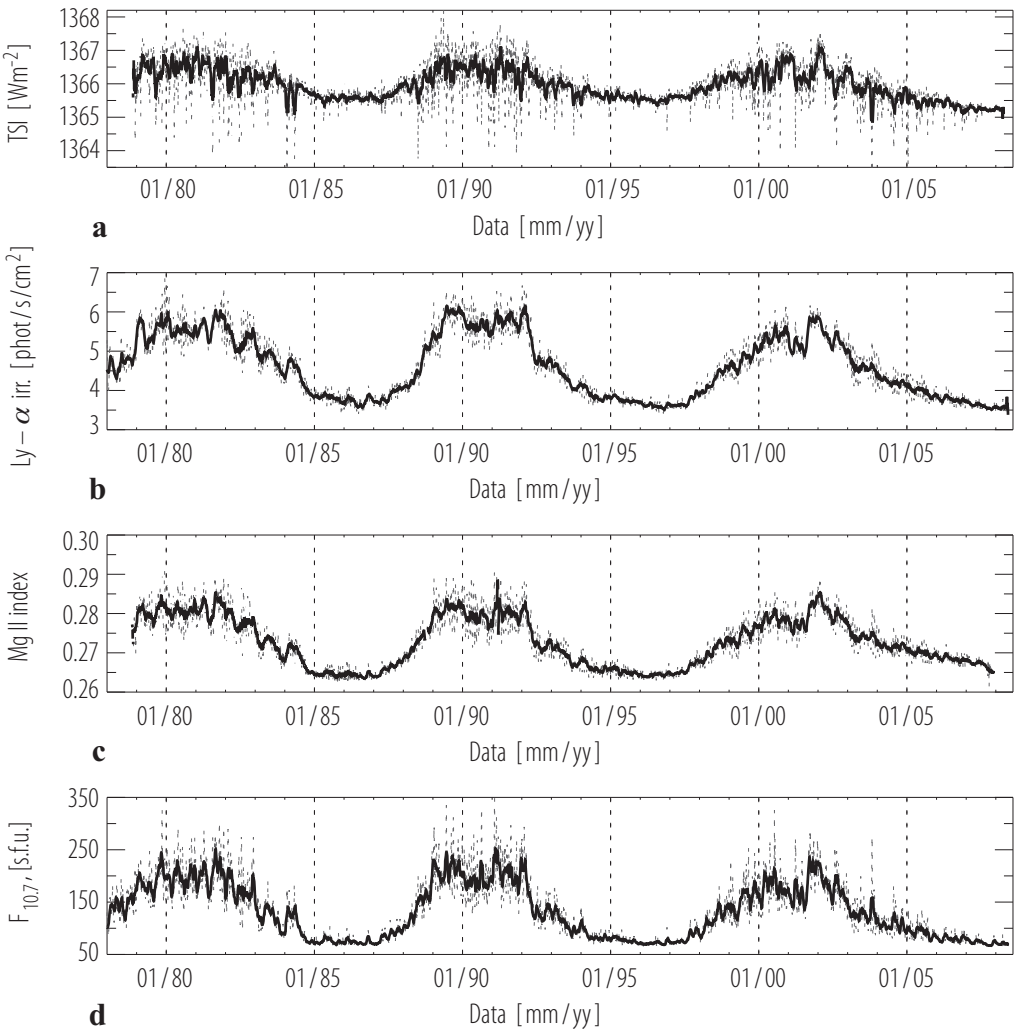

Fig. 6. Solar total (a) and Ly-α (b) irradiance, the Mg II index (c) and the 10.7 cm radio flux (d) for cycles 21-23. The dotted and solid lines show daily and monthly averaged values, respectively.

irradiance measurements. The Mg II index (Fig. 6c; data from [04Vie]) is a good measure of solar UV and EUV emission.

Another widely used indicator of the magnetic activity of the Sun and solar-type stars is the emission in the core of the Ca II H (396.85 nm) and K (393.36 nm) doublet [e, 98Whi], which brightens in areas with increased magnetism. Long-term monitoring programmes of Ca II profiles have been carried out by the National Solar Observatory (NSO) on Kitt Peak [81Whi] and at Sacramento Peak [98Kei] since 1974 and 1976, respectively.

Solar emission at 2800 MHz or 10.7 cm [47Cov, d] originates from the upper chromosphere and lower corona. Solar flux at 10.7 cm integrated over the entire solar disc has been recorded routinely by the National Research Council of Canada since February 14, 1947. The data are available from NGDC [08Nat]. The 10.7 cm flux, $F_{10.7}$, correlates well with the sunspot number and area, Ca II and Mg II indices, the full-disc X-ray flux, as well as with the solar total and UV irradiance (Fig. 6d; data from [08Nat]). This agreement between different indices originating in different parts of the solar atmosphere and produced by different emission mechanisms points to their modulation by a common source, the solar magnetic field [94Tap].

4.1.2.2.4 Longer term variations and secular change

Different historic proxies of solar magnetic activity, e.g., sunspot data, auroral and geomagnetic records, as well as cosmogenic isotope concentrations in natural archives, suggest that it also varies on longer time scales [76Edd, 80Sis, 84Kri, 99Loc]. There are periods of generally higher or lower activity.

For example, during the 17th century there was an extended period (around 1645-1715), the Maunder minimum, when hardly any spots appeared on the solar surface [76Edd, c]. The 11-a cycle was suppressed, whereas the 22-a Hale cycle can still be detected in the sunspot data [00Uso]. Records of other proxies suggest that the activity did not cease completely during the Maunder minimum but continued at a significantly lower level [92Sil, 98Bee, 04Miy]. The 11-a magnetic activity cycle persisted although apparently became longer, up to about 13-15 years [81Zel, 92Sch, 92Sil, 98Bee, 99Fli, 04Miy] (see Table 1).

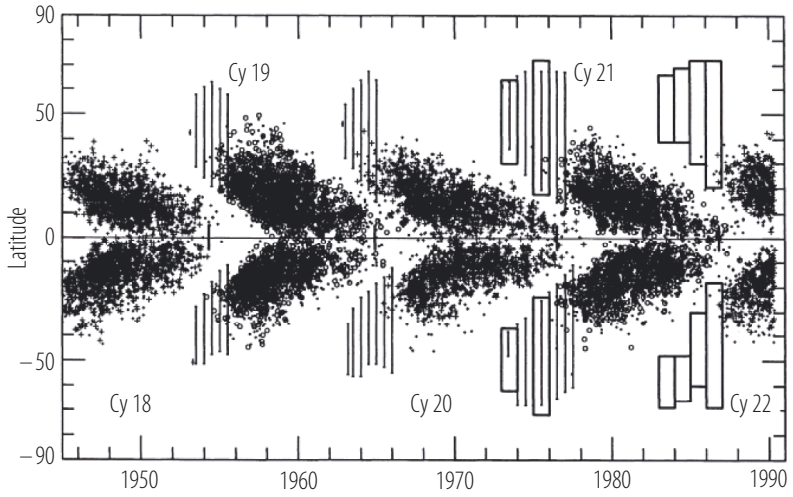

Fig. 7. Butterfly diagram of sunspot regions (plus signs and circles for even and odd cycles, respectively) combined with latitudinal extent of Ca^+ plage regions (vertical lines) and ephemeral regions (boxes) identified with new cycles [b]. The cycle minima are indicated by vertical lines.

On average, solar activity has increased since the Maunder minimum. The trend is seen to some extent in the sunspot number (see Fig. 1), but is even more prominent in geomagnetic activity, auroral or cosmogenic isotope records [90Bee, 92Sil, 07Rou]. In particular, between 1903 and 1956, the open solar flux increased by about 70-100%, the mean interplanetary magnetic field strength by 45.1±4.5% and the solar wind speed by 14.4±0.7% [99Loc, 07Rou]. The production rate of ^{14}C decreased by about 30% from the Maunder minimum to the beginning of the 20th century [80Stu]. The concentration of ^{10}Be in polar ice almost doubled from 1880 to 1960 [90Bee].

The origin of the trend has been explained within the concept of 'extended' activity cycles [00Sol, 02Sol]. At sunspot minima, sunspots belonging to both, preceeding and incipient, cycles are observed [79Spo, 92Har, c]. They can be distinguished by their latitudes and polarity. The time interval between the first and last observed sunspot region belonging to the same activity cycle is several years longer than the interval between the successive minima (Figs. 2 and 7). The duration of the sunspot activity in cycles 14-20 was found to be around 13-14 years, 1.8-3.3 years longer than the time interval between successive sunspot minima [92Har]; cf. Fig. 2. Yet earlier onset and later end times of a particular cycle are observed for smaller bipolar regions (Fig. 7; [92Har]). Magnetic activity belonging to cycle 21 could be traced for about 18-22 years [88Wil].

From the green (5303 Å) coronal line emission data for 1940-1989, the length of the global coronal activity cycles was estimated to be 16-18 years [92Bor]. Thus consecutive activity cycles overlap by about 3-5 years, and the extended period during which activity of a given cycle occurs is called the extended activity cycle [88Wil].

An overlap between consecutive cycles implies that the flux does not drop to zero at activity minimum (Figs. 3 and 7) building up background magnetic flux, whose level varies with time and leads to a secular variation in solar irradiance [00Sol, 02Sol]. A model based on the concept of extended activity cycles explains the increase by almost a factor of 2 of the solar open magnetic flux since the beginning of the 20th century inferred from combinations of geomagnetic indices [99Loc, 07Rou] and predicts an increase in the cycle-averaged TSI since the Maunder minimum of $1.3^{+0.2}_{-0.4}\,\mathrm{Wm}^{-2}$ [07Kri].

Solar activity can to some extent be followed further back in time with sunspot, auroral or geomagnetic activity records [55Sch, 80Sis, 84Kri, 07Vaq]. On millennial time scales, it is best traced back using cosmogenic isotope data. The production rate of cosmogenic radioisotopes is modulated by the interaction of the solar wind with galactic cosmic ray particles and thus provides information on the Sun's magnetic activity. The two cosmogenic isotopes most widely used to trace solar activity are ^{14}C and ^{10}Be [80Stu, 89Stu, 90Bee]. [04Sol, 04Uso] have combined physics-based models for each of the processes connecting ^{14}C and ^{10}Be concentration with sunspot number and

Table 3. Approximate dates (in –BC/AD) of grand minima in reconstructed solar activity [07Uso].

No.	Center	Duration	Name
1	1680	80	Maunder
2	1470	160	Spörer
3	1305	70	Wolf
4	1040	60	Oort
5	685	70	
6	–360	60	
7	–765	90	
8	–1390	40	
9	–2860	60	
10	–3335	70	
11	–3500	40	
12	–3625	50	
13	–3940	60	
14	–4225	30	
15	–4325	50	
16	–5260	140	
17	–5460	60	
18	–5620	40	
19	–5710	20	
20	–5985	30	
21	–6215	30	
22	–6400	80	
23	–7035	50	
24	–7305	30	
25	–7515	150	
26	–8215	110	
27	–9165	150	

Table 4. Approximate dates (in –BC/AD) of grand maxima in reconstructed solar activity [07Uso].

No.	Center	Duration
1[a]	1960	80
2	–445	40
3	–1790	20
4	–2070	40
5	–2240	20
6	–2520	20
7	–3145	30
8	–6125	20
9	–6530	20
10	–6740	100
11	–6865	50
12	–7215	30
13	–7660	80
14	–7780	20
15	–7850	20
16	–8030	50
17	–8350	70
18	–8915	190
19	–9375	130

[a] Center and duration of the modern maximum are preliminary since it is still ongoing.

reconstructed the sunspot number for the whole Holocene.

Records of cosmogenic isotope concentrations and aurorae suggest that prolonged periods of very low solar magnetic activity like during the Maunder minimum have regularly occured in the past. Such periods are called grand minima. Two kinds of grand minima have been identified: shorter (30-90 a) Maunder-type events and longer (> 110 a) Spörer-type events [89Stu, 07Uso]. Evidence indicates that periods of higher averaged solar activity, similar to the recent one started around 1930, called grand maxima, have also occurred [07Uso]. Approximate dates and duration of grand minima and maxima over the Holocene [07Uso] are listed in Tables 3 and 4. During the Holocene, the Sun spent about 3/4 of the time at moderate magnetic activity levels and about 17% and 9-22% of the time in grand minima and grand maxima, respectively [07Uso].

Overall solar activity has been found to vary on a characteristic time scale of about 200 years (de Vries or Suess cycle; [55Sch, 76Edd, 89Stu, 96Vos, 01Wag]). Another quasi-periodicity widely detected in various proxies is the Gleissberg cycle at around 80-90 years [39Gle, 55Sch, 84Fey, 03Per]. However, the occurrence of grand minima and maxima does not display any significant periodicity. Rather grand minima and maxima are often bunched together, with the bunches being separated by longer periods of time [07Uso].

4.1.2.2.5 References for 4.1.2.2

General references

a Balogh, A., Lanzerotti, L.J., Suess, S.T.: The Heliosphere through the Solar Activity Cycle, New York: Springer Praxis Books (2008).

b Harvey, K.L.: Magnetic dipoles on the Sun, PhD Thesis, Univ. Utrecht (1993).

c Kippenhahn, R.: Discovering the Secrets of the Sun, Chichester: Wiley (1984).

d Kundu, M.R.: Solar radio astronomy, New York: Interscience Publication (1965).

e Livingston, W., White, O.R.: Allen's Astrophysical Quantities (A.N. Cox, ed.), New York: Springer (2000) 351.

f Stix, M.: The Sun: An Introduction, Berlin: Springer (2004).

Special references

19Hal Hale, G.E., Ellerman, F., Nicholson, S.B., Joy, A.H.: Astrophys. J. **49** (1919) 153.

35Wal Waldmeier, M.: Astron. Mitteil. Zürich **14** (1935) 105.

39Gle Gleissberg, W.: The Observatory **62** (1939) 158.

44Sch Schwabe, H.: Astronomische Nachrichten **21, No. 495** (1844) 233.

47Cov Covington, A.E.: Nature **159** (1947) 405.

48Gne Gnevyshev, M.N., Ohl, A.I.: Astron. Zh. **25** (1948) 18.

55Sch Schove, D.J.: J. Geophys. Res. **60** (1955) 127.

58Car Carrington, R.C.: Mon. Not. Royal Astron. Soc. **19** (1858) 1.

76Edd Eddy, J.A.: Science **192** (1976) 1189.

76Liv Livingston, W.C., Harvey, J., Pierce, A.K., Schrage, D., Gillespie, B., Simmons, J., Slaughter, C.: Applied Optics **15** (1976) 33.

77Sch Scherrer, P.H., Wilcox, J.M., Svalgaard, L., Duvall, T.L., Jr., Dittmer, P.H., Gustafson, E.K.: Solar Physics **54** (1977) 353.

79Spo Spoerer, F.W.G.: Astronomische Nachrichten **94** (1879) 173.

80Sis Siscoe, G.L.: Reviews of Geophysics and Space Physics **18** (1980) 647.

80Stu Stuiver, M., Quay, P.D.: Science **207** (1980) 11.

81Whi White, O.R., Livingston, W.C.: Solar Physics **249** (1981) 798.

81Zel Zeller, E.J., Parker, B.C.: Geophys. Res. Lett. **8** (1981) 895.
84Fey Feynman, J., Fougere, P.F.: J. Geophys. Res. **89** (1984) 3023.
84Kri Krivsky, L.: Solar Physics **93** (1984) 189.
85How Howard, R.: Solar Physics **100** (1985) 171.
88Wil Wilson, P.R., Altrock, R.C., Harvey, K.L., Martin, S.F., Snodgrass, H.B.:Nature **333** (1988) 748.
89Stu Stuiver, M., Braziunas, T.F.: Nature **338** (1989) 405.
90Bee Beer, J., Blinov, A., Bonani, G., Hofmann, H.J., Finkel, R.C.: Nature **347** (1990) 164.
91How Howard, R.F.: Solar Physics **132** (1991) 49.
92Bor Bortsov, V.V., Makarov, V.I., Mikhailutsa, V.P.: Solar Physics **137** (1992) 395.
92Har Harvey, K.L.: The solar cycle, ASP Conf. Ser. **27** (1992) 335.
92Sch Schröder, W.: J. Geomag. Geoelectr. **44** (1992) 119.
92Sil Silverman, S.M.: Reviews of Geophysics **30** (1992) 333.
94Hat Hathaway, D.H., Wilson, R.M., Reichmann, E.J.: Solar Physics **151** (1994) 177.
94Tap Tapping, K.F., Harvey, K.L.: The Sun as a Variable Star: Solar and Stellar Irradiance Variations, IAU Colloq. **143** (1994) 182.
96Vos Voss, H., Kurths, J., Schwarz, U.: J. Geophys. Res. **101** (1996) 15637.
98Bee Beer, J., Tobias, S., Weiss, N.: Solar Physics **181** (1998) 237.
98Hoy Hoyt, D.V., Schatten, K.H.: Solar Physics **181** (1998) 491.
98Kei Keil, S.L., Henry, T.W., Fleck, B.: Synoptic Solar Physics, ASP Conf. Ser. **140** (1998) 301.
98Whi White, O.R., Livingston, W.C., Keil, S.L., Henry, T.W.: Synoptic Solar Physics, ASP Conf. Ser. **140** (1998) 293.
99Fli Fligge, M., Solanki, S.K., Beer, J.: Astron. Astrophys. **346** (1999) 313.
99Loc Lockwood, M., Stamper, R., Wild, M.N.: Nature **399** (1999) 437.
00Sol Solanki, S.K., Schüssler, M., Fligge, M.: Nature **408** (2000) 445.
00Unr Unruh, Y.C., Solanki, S.K., Fligge, M.: Sp. Sci. Rev. **94** (2000) 145.
00Uso Usoskin, I.G., Mursula, K., Kovaltsov, G.A.: Astron. Astrophys. **354** (2000) L33.
00Woo Woods, T.N., Tobiska, W.K., Rottman, G.J., Worden, J.R.: J. Geophys. Res. **105** (2000) 27195.
01Hag Hagenaar, H.J.: Astrophys. J. **555** (2001) 448.
01Wag Wagner, G., Beer, J., Masarik, J., Muscheler, R., Kubik, P.W., Mende, W., Laj, C., Raisbeck, G.M., Yiou, F.: Geophys. Res. Lett. **28** (2001) 303.
02Arg Arge, C.N., Hildner, E., Pizzo, V.J., Harvey, J.W.: J. Geophys. Res. **107** (2002) DOI: 10.1029/2001JA000503.
02Hat Hathaway, D.H., Wilson, R.M., Reichmann, E.J.: Solar Physics **211** (2002) 357.
02Sol Solanki, S.K., Schüssler, M., Fligge, M.: Astron. Astrophys. **383** (2002) 706.
03Flo Floyd, L.E., Cook, J.W., Herring, L.C., Crane, P.C.: Adv. Space Res. **31** (2003) 2111.
03Hag Hagenaar, H.J., Schrijver, C.J., Title, A.M.:Astrophys. J. **584** (2003) 1107.
03Hat Hathaway, D.H.: Proc. of SOHO 12/GONG+ 2002 'Local and GlobalHelioseismology: The Present and Future', ESA SP-**517** (2003) 87.
03Per Peristykh, A.N., Damon, P.E: J. Geophys. Res. **108** (2003) DOI:10.1029/2002JA009390.
03Sol Solanki, S.K., Krivova, N.A., Schössler, M., Fligge, M.: Astron. Astrophys. **396** (2003) 1029.
04Kri Krivova, N.A., Solanki, S.K.:Astron. Astrophys. **417** (2004) 1125.
04Mau Maunder, E.W.: Mon. Not. Royal Astron. Soc. **64** (1904) 747.
04Miy Miyahara, H., Masuda, K., Muraki, Y., Furuzawa, H., Menjo, H., Nakamura, T.: Solar Physics **224** (2004) 317.
04Sol Solanki, S.K., Usoskin, I.G., Kromer, B., Schüssler, M., Beer, J.: Nature **431** (2004) 1084.

04Uso Usoskin, I.G., Mursula, K., Solanki, S.K., Schüssler, M., Alanko, K.: Astron. Astrophys. **413** (2004) 745.
04Vie Viereck, R.A., Floyd, L.E., Crane, P.C., Woods, T.N., Knapp, B.G., Rottman, G., Weber, M., Puga, L.C., DeLand, M.T.: Space Weather **2** (2004) DOI: 10.1029/2004SW000084.
05Bal Balmaceda, L., Solanki, S.K., Krivova, N.A.: Mem. Soc. Astron. It. **76** (2005) 929.
06Fro Fröhlich, C.: Space Sci. Rev. **125** (2006) 53.
06Kri Krivova, N.A., Solanki, S.K., Floyd, L.: Astron. Astrophys. **452** (2006) 631.
06Wen Wenzler, T., Solanki, S.K., Krivova, N.A., Fröhlich, C.: Astron. Astrophys. **460** (2006) 583.
07Cha Charbonneau, P., Beaubien, G., St-Jean, C.: Astrophys. J. **658** (2007) 657.
07Kri Krivova, N.A., Balmaceda, L., Solanki, S.K.: Astron. Astrophys. **467** (2007) 335.
07Rou Rouillard, A.P., Lockwood, M., Finch, I.: J. Geophys. Res. **112** (2007) DOI: 10.1029/2006JA012130.
07Uso Usoskin, I.G., Solanki, S.K., Kovaltsov, G.A.: Astron. Astrophys. **471** (2007) 301.
07Vaq Vaquero, J.M.: Advances in Space Research **40** (2007) 929.
08Dik Dikpati, M., Gilman, P.A., de Toma, G.: Astrophys. J. **673** (2008) L99.
08Nat National Geophysical Data Center (NGDC). Solar Data Services: http://www.ngdc.noaa.gov/stp/SOLAR/solar.html; cited on May 29,2008.
08Sol Solanki, S.K., Wenzler, T., Schmitt, D.: Astron. Astrophys. **483** (2008) 623.